Regional apparent density correlations within the proximal humerus

Jacob M. Reeves, PhD[a,*], Tom Vanasse, MSE[b], Chris Roche, MSE, MBA[b],
George S. Athwal, MD, FRCSC[c], James A. Johnson, PhD[a], Kenneth J. Faber, MD, FRCSC[c],
G. Daniel G. Langohr, PhD[a]

[a] University of Western Ontario, London, ON, Canada
[b] Exactech., Gainesville, FL, USA
[c] Roth|McFarlane Hand and Upper Limb Clinic, London, ON, Canada

A R T I C L E   I N F O

Keywords:
Shoulder arthorplasty
Apparent density
Proximal humerus
Density correlation
Apparent bone density
Thumb test
Bone quality

Level of evidence: Anatomy study; Imaging

Background: Bone quality influences humeral implant selection for shoulder arthroplasty. However, little is known about how well bone near the humeral resection represents more distal cancellous bone. This investigation aimed to quantify the correlations between the apparent density of sites near the humeral head resection plane and cancellous sites throughout the metaphysis.
Methods: Using computed tomography data from 98 subjects, apparent bone density was quantified in 65 regions throughout the proximal humerus. Pearson's correlation coefficient was determined comparing the density between samples from the humeral resection and all supporting regions beneath the resection. Mean correlation coefficients were compared for (i) each sample region with all support regions, (ii) pooling all sample regions within a slice, and (iii) considering sample regions correlated with only the support regions in the same anatomic section.
Results: Stronger correlations existed for bone sampled beneath the resection ($0.33 \pm 0.10 \leq r \leq 0.88 \pm 0.10$), instead of from the resected humeral head ($0.22 \pm 0.10 \leq r \leq 0.66 \pm 0.14$). None of sample region correlated strongly with all support regions; however, strong correlations existed when sample and support regions both came from the same anatomic section.
Discussion: Assessments of cancellous bone quality in the proximal humerus should be made beneath the humeral resection not in the resected humeral head; and each anatomic quadrant should be assessed independently.

Introduction

Shoulder arthroplasty has become an effective surgical treatment for osteoarthritis (OA), inflammatory arthritis, fracture, and cuff tear arthropathy. The incidence of shoulder arthroplasty is on the rise, and current trends show no indication of its use being decreased.[15] In a recent global assessment, Lübbeke et al found the incidence of shoulder arthroplasty increased from 5 to 13 people per 10^5 of the population from 2002 to 2012, where the data were available (ie, Norway, Sweden, and New Zealand). Similarly, in the United States, the number of shoulder arthroplasty cases per year has increased from 47,000 in 2008[13] to 66,000 in 2011[23] and is projected to reach 188,000 in 2025.[7]

The number of commercially available shoulder arthroplasty implants has grown alongside this demand. A variety of traditional, short, and stemless humeral components have been approved for use; each of which relies on varying degrees of support from the metaphyseal cancellous bone. Shoulder surgeons now have several options regarding implant selection, sizing, and technique; all of which must be balanced in pursuit of the most favorable outcome. An objective metric may assist surgeons with implant selection and fixation method to optimize and personalize care for a given patient. Premature implant failure seems to be influenced at least in part by poor primary stability at the time of surgery, prosthesis loosening, instability, and periprosthetic fracture.[3,4,9] Improving initial implant stability reduces micromotion at the implant-bone interface and promotes implant osseointegration.[12]

In balancing these many factors and selecting the appropriate implant for a patient, shoulder surgeons often rely on a subjective assessment of bone quality, colloquially called the "thumb test." During this test, the surgeon infers bone quality by applying thumb pressure to the cancellous bone of one or both surfaces of the humeral head resection plane and subjectively gauging the bone's

resistance to deformation.[17] Not surprisingly, similar subjective manual touch assessments of bone quality have been shown to diverge among surgeons and depend greatly on surgical experience.[28] Subjective tactile assessments of bone quality can be supplemented with tools such as the osteopenetrometer[11,24] and the DensiProbe[10,18,25,26] that collect objective data on bone quality in the spine, hip and knee, though neither is commonly used in shoulder arthroplasty.

Bone mineral density is an objective surrogate metric of bone quality, which has been shown to predict approximately 60%-70% of bone strength variations.[1] However, before a tool is developed to assess the bone that is readily available at the resection surface, it is important to know if the local bone quality available for measurement at the resection surface correlates well with the cancellous sites that ultimately support humeral implants throughout the metaphysis because cancellous bone is known to have regionally varying inhomogeneous material properties.[2,27,29]

While a previous investigation of patient and cadaveric computed tomography (CT) scans has quantified the regional apparent density variations that occur within the proximal humerus,[20] these data have not been assessed for its intra-site correlations, and it is unknown how well the resection-site bone density variations correlate with changes in the remaining metaphyseal bone.

The purpose of this investigation was to quantify the correlations that may exist between the apparent density of sample sites near the humeral head resection plane and the support sites that remain to interface with an implanted humeral stem. It was hypothesized that bone density sampled distal to the resection will correlate better with the support regions than that sampled proximal to the resection (ie, the resected humeral head) and that correlations will be stronger between sample and support regions that lie within the same anatomic section (ie, anterior sample to correlate best with anterior support, and so on).

Materials and methods

The CT scans from 98 subjects were classified as per their glenohumeral OA condition by a shoulder surgeon (G.S.A.) with 15 years of experience, using a method that has demonstrated clinical reliability (Nowak 2010, Walch 1999). Subjects' humeral heads were categorized as either nonarthritic (25 men: 71 ± 16 years; 16 women: 70 ± 12 years), Walch type A (symmetric) osteoarthritic (15 men: 62 ± 11 years; 16 women: 69 ± 14 years), or Walch type B2 (anterior erosion) osteoarthritic (11 men: 64 ± 11 years; 15 women: 69 ± 7 years). The CT scans for the OA cohorts were from a patient population, while the nonarthritic scans were obtained from a cadaveric population. Ethics approval was granted by the appropriate institutional review board.

Mimics research software (Materialise Inc; Plymouth, MI, USA) was used to reconstruct the Digital Imaging and Communications in Medicine CT scan data and to isolate the voxels corresponding to humeral tissue of interest using the software's masking features. Each humeral mask was then separated into an external cortical component and the remaining internal cancellous bone and humeral canal. The surgeon (G.S.A.) then virtually selected several landmarks on the humeral head, as well as the most superior-lateral and inferior-medial points on the resection surface, to define a surgical resection plane. Together, these points were used to construct a consistent humeral coordinate system with the x- and y-axes on the resection plane, directed toward the lateral and anterior sides of the humerus, respectively, and the z-axis directed distally into, and perpendicular to, the resection plane (Fig. 1). The internal section of the humerus containing the cancellous bone and canal was then exported as a 4-dimensional point cloud including CT attenuation (ie, [x, y, z, HU]).

Each point cloud was then analyzed using a custom LabVIEW code (National Instruments; Austin, TX, USA). The CT attenuation data (HU) was linearly calibrated[22] and converted into apparent density (g/cm^3). The program also divided the internal section of each humerus into 13 slices that were 5-mm thick and parallel to the humeral head resection plane (3 above the resection, 10 beneath the resection). The geometric center of each slice was then used to further subdivide the bone into five anatomic regions including a central circular section with diameter equal to half of the canal diameter and four 90° peripheral sections centered about the anterior, posterior, medial, and lateral sides of the humerus (Fig. 2). The average apparent density (ρ_{AVG}) was then quantified for each subsection of the cancellous bone and canal. These densities have previously been reported,[20] but a summary is presented in Table I.

The average density of each anatomic region within the two slices directly proximal to and distal to the resection plane (ie, sample regions) was correlated with the density quantified in each anatomic region of all slices beneath the resection plane (ie, support regions). Correlations were performed using Microsoft Excel's data analysis package (Microsoft Corporation; Redmond, WA, USA), and Pearson's correlation coefficient (r) was determined for each sample-support section pair. Previous work has demonstrated that the greatest cancellous bone density lies in the first 20 mm beneath the resection plane, suggesting that this region plays an important role in supporting implants after shoulder arthroplasty.[20] Accordingly, each support region was further classified as being either proximal (0-20 mm beneath the resection) or distal (20-50 mm beneath the resection). The division of sample and support regions is shown in Figure 2.

To determine if any one anatomic region correlated best with the support regions, the mean and standard deviation of the Pearson's correlation coefficient were then quantified between each anatomic sample region independently with all support regions. Similarly, to test if a whole sample slice would correlate well with the support regions, the mean correlation coefficients were then quantified for all anatomic regions pooled together within each sample bone slice (ie, all together). Finally, to determine if comparisons were improved if sample and support regions were taken from the same anatomic sections, the mean of the correlation coefficients was quantified for each slice only considering sample-support region pairs that were within the same anatomic section (ie, anatomically paired). Correlation strength was assessed to be strong for $r \geq 0.7$, moderate for $0.7 > r > 0.3$, and weak for $r \leq 0.3$.

Results

Individual sample-to-support site density correlation coefficients found from pooling the subjects together are presented in Supplementary Figures S1-S4, with Tables II and III summarizing the mean and standard deviation values for all demographics. Regardless of arthritic classification, better apparent density correlations were found when the bone distal–to–the humeral head resection plane was used as the sample region ($0.33 \pm 0.10 \leq r \leq 0.88 \pm 0.10$), as opposed to the bone proximal to the resection in the resected humeral head ($0.22 \pm 0.10 \leq r \leq 0.66 \pm 0.14$). Correlations with the distal support region (ie, 20-50 mm beneath the resection) were generally poor ($r \leq 0.3$) to moderate ($0.3 < r < 0.7$) regardless of which sample region was used; however, several strong ($r \geq 0.7$) correlations were found with the proximal support region.

Comparisons made using a single anatomic sample region

The correlation strengths found between any 1 anatomic sample region and all support regions were mixed ($-0.03 \pm 0.20 \leq r \leq 0.80 \pm 0.11$), with none strongly correlated for B2 OA subjects
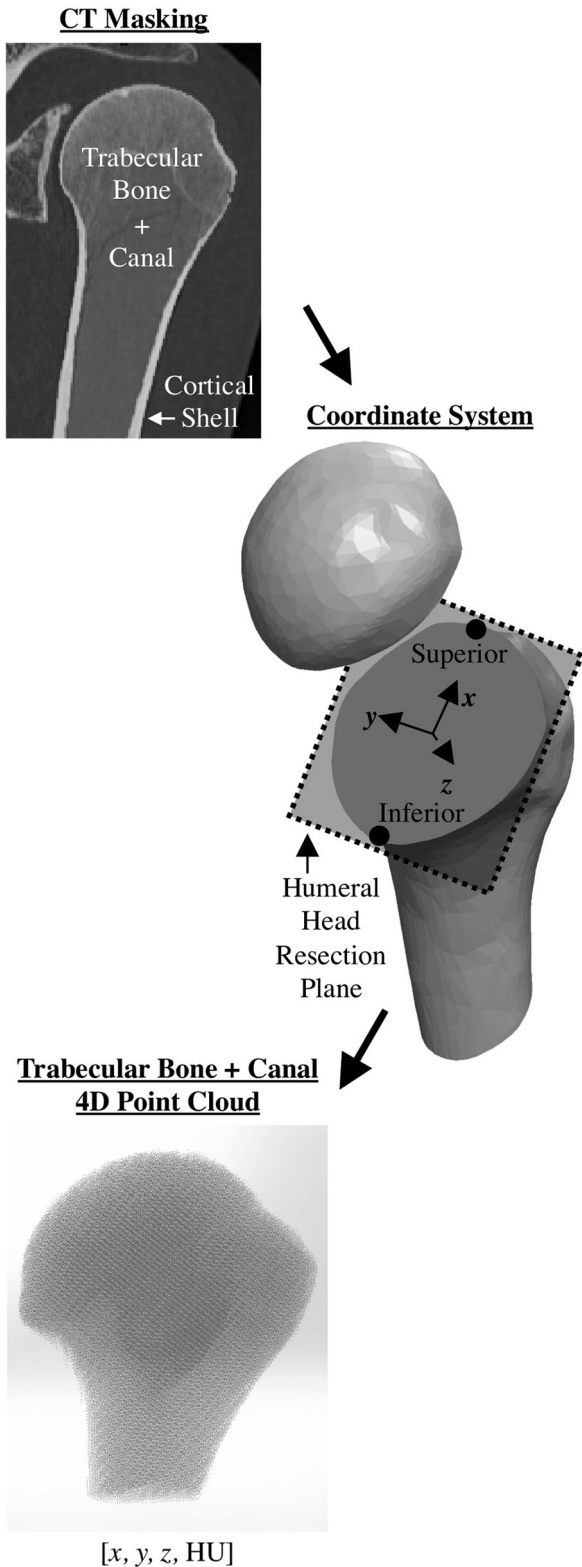
CT Masking

Coordinate System

Trabecular Bone + Canal
4D Point Cloud

[x, y, z, HU]

Figure 1 Visual progression of the data segmentation from CT masking to humeral coordinate system construction and 4D point cloud development for data analysis. *CT*, computed tomography.

(r ≤ 0.63 ± 0.27). The anatomic sample regions that produced the strongest and weakest correlations with the proximal support region changed depending on which bone slice was sampled (Tables II and III). At 5-10 mm proximal to the resection plane, the
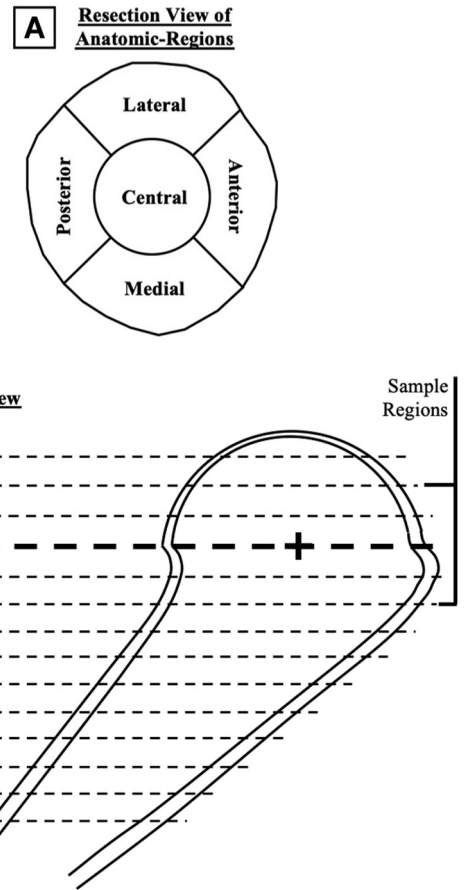

Figure 2 Visualization of the subdivision into the 5 anatomic regions of interest (**A**) and the division of the proximal humerus into the thirteen 5-mm slices parallel to the humeral head resection plane (**B**). Note the sample region, as well as the division between proximal and distal support regions in part B.

strongest correlations were found in the lateral section (r = 0.55 ± 0.10) and the weakest in the posterior section (r = 0.48 ± 0.12). Using the slice 0-5 mm proximal to the resection, the best correlations also came from the lateral region (r = 0.62 ± 0.14) and the poorest from the anterior region (r = 0.51 ± 0.13). Distal to the resection plane, from 0 to 5 mm, the best correlations came from the central region (r = 0.70 ± 0.11), while the worst were from the anterior region (r = 0.60 ± 0.14). Finally, samples taken from 5 to 10 mm distal to the resection were strongest using the posterior region (r = 0.72 ± 0.12) and weakest using the medial region (r = 0.64 ± 0.14).

Comparisons made from all sample regions pooled together in each slice

Similar trends in correlation strength persisted when the correlations from all anatomic regions were pooled across each sample slice to assess the proximal support region's apparent density (Tables II and III). Again, pooling the OA conditions, the correlations were stronger for the sample regions distal to the resection plane (0-5 mm below: r = 0.65 ± 0.14; 5-10 mm below: r = 0.67 ± 0.14), as opposed to those proximal to the resection plane (5-10 mm above: r = 0.51 ± 0.09; 0-5 mm above: r = 0.56 ± 0.12).

Comparisons made considering anatomically paired regions

Regardless of which slice was used as the sample slice and which OA classification the subjects belonged to, the strongest

Table I
Mean (standard deviation) apparent density data [g/cm^3] from all 98 subjects pooled together and broken down as per anatomic section and slice depth in 5-mm increments relative to the humeral head resection plane.

	Slice depth [mm]	Trabecular bone apparent density [g/cm^3]				
		Anterior	Posterior	Medial	Lateral	Central
		Mean (SD)	Mean (SD)	Mean (SD)	Mean (SD)	Mean (SD)
Above resection	+10 to 15	0.35 (0.10)	0.36 (0.12)	0.38 (0.10)	0.34 (0.11)	0.32 (0.10)
	+5 to 10	0.24 (0.08)	0.24 (0.10)	0.28 (0.08)	0.24 (0.09)	0.21 (0.08)
	+0 to 5	0.17 (0.06)	0.16 (0.07)	0.21 (0.06)	0.18 (0.06)	0.18 (0.07)
Below resection	−0 to 5	0.14 (0.05)	0.13 (0.05)	0.17 (0.05)	0.15 (0.05)	0.12 (0.06)
	−5 to 10	0.12 (0.04)	0.12 (0.05)	0.17 (0.06)	0.13 (0.04)	0.06 (0.04)
	−10 to 15	0.13 (0.04)	0.11 (0.05)	0.15 (0.06)	0.12 (0.04)	0.04 (0.02)
	−15 to 20	0.13 (0.04)	0.12 (0.05)	0.11 (0.06)	0.11 (0.04)	0.03 (0.02)
	−20 to 25	0.12 (0.06)	0.12 (0.05)	0.08 (0.05)	0.11 (0.04)	0.03 (0.03)
	−25 to 30	0.11 (0.06)	0.11 (0.05)	0.08 (0.04)	0.11 (0.05)	0.03 (0.02)
	−30 to 35	0.10 (0.06)	0.10 (0.06)	0.08 (0.04)	0.11 (0.05)	0.02 (0.02)
	−35 to 40	0.09 (0.06)	0.09 (0.05)	0.08 (0.04)	0.10 (0.05)	0.02 (0.02)
	−40 to 45	0.09 (0.05)	0.09 (0.06)	0.08 (0.05)	0.10 (0.05)	0.02 (0.02)
	−45 to 50	0.09 (0.05)	0.09 (0.06)	0.08 (0.05)	0.10 (0.05)	0.02 (0.01)

Table II
Mean (standard deviation) of Pearson's coefficients of correlation between each sample region and the proximal support region that lies 0-20 mm beneath the humeral head resection, broken down as per sample slice depth, anatomic region and pooling technique, as well as subject osteoarthritis classification.

Pearson's coefficient of correlation with the proximal support region (0-20 mm)					
Sample slice	Anatomic region	Pooled demographics	Non-arthritic	B2 OA	Symmetric OA
		Mean (SD)	Mean (SD)	Mean (SD)	Mean (SD)
5-10 mm above resection	Anterior	0.49 (0.08)	0.46 (0.16)	0.11 (0.18)	0.68 (0.07)
	Posterior	0.48 (0.12)	0.58 (0.12)	0.39 (0.22)	0.46 (0.07)
	Medial	0.49 (0.05)	0.52 (0.13)	0.36 (0.22)	0.63 (0.08)
	Lateral	0.55 (0.10)	0.54 (0.16)	0.29 (0.16)	0.70 (0.10)
	Central	0.54 (0.11)	0.69 (0.13)	0.22 (0.14)	0.62 (0.07)
	All pooled	0.51 (0.09)	0.56 (0.16)	0.28 (0.21)	0.62 (0.11)
	Anatomically paired	0.57 (0.10)	0.57 (0.16)	0.40 (0.19)	0.66 (0.11)
0-5 mm above resection	Anterior	0.51 (0.13)	0.58 (0.18)	0.07 (0.28)	0.66 (0.08)
	Posterior	0.58 (0.12)	0.64 (0.14)	0.50 (0.22)	0.64 (0.09)
	Medial	0.52 (0.07)	0.63 (0.12)	0.33 (0.19)	0.57 (0.12)
	Lateral	0.62 (0.11)	0.65 (0.16)	0.44 (0.17)	0.73 (0.08)
	Central	0.58 (0.15)	0.68 (0.15)	0.36 (0.22)	0.73 (0.08)
	All pooled	0.56 (0.12)	0.63 (0.15)	0.34 (0.26)	0.67 (0.11)
	Anatomically paired	0.66 (0.14)	0.66 (0.15)	0.54 (0.19)	0.76 (0.09)
0-5 mm below resection	Anterior	0.60 (0.14)	0.73 (0.15)	0.27 (0.30)	0.67 (0.13)
	Posterior	0.67 (0.13)	0.75 (0.12)	0.58 (0.28)	0.70 (0.13)
	Medial	0.60 (0.13)	0.64 (0.16)	0.46 (0.21)	0.66 (0.12)
	Lateral	0.68 (0.14)	0.75 (0.16)	0.62 (0.20)	0.69 (0.13)
	Central	0.70 (0.11)	0.76 (0.10)	0.56 (0.21)	0.78 (0.09)
	All pooled	0.65 (0.14)	0.73 (0.14)	0.50 (0.27)	0.70 (0.13)
	Anatomically paired	0.82 (0.14)	0.84 (0.15)	0.79 (0.18)	0.85 (0.11)
5-10 mm below resection	Anterior	0.65 (0.13)	0.77 (0.14)	0.31 (0.29)	0.72 (0.11)
	Posterior	0.72 (0.12)	0.80 (0.11)	0.63 (0.27)	0.74 (0.11)
	Medial	0.64 (0.14)	0.56 (0.19)	0.57 (0.16)	0.78 (0.11)
	Lateral	0.65 (0.16)	0.68 (0.19)	0.62 (0.23)	0.65 (0.16)
	Central	0.71 (0.11)	0.69 (0.13)	0.61 (0.25)	0.79 (0.10)
	All pooled	0.67 (0.14)	0.70 (0.17)	0.55 (0.27)	0.74 (0.13)
	Anatomically paired	0.88 (0.10)	0.89 (0.10)	0.84 (0.14)	0.91 (0.08)

correlations were found when each anatomic sample region was compared only with the same anatomic section of the proximal support regions (Tables II and III); for example, when the anterior sample region was compared with the anterior support region. For B2 OA subjects, the anatomically paired correlations ranged from 0.40 ± 0.19 to 0.84 ± 0.14, depending on sample slice depth. Similarly, for type A OA subjects, the anatomic correlations ranged from 0.66 ± 0.11 to 0.91 ± 0.08, and for nonarthritic subjects, the anatomic correlations ranged from 0.57 ± 0.16 to 0.89 ± 0.10, depending on sample slice depth.

Discussion

Substantial differences presented between sample and support site apparent bone density correlations depended on which resection site was sampled and whether that site was compared with the entire support region or only its anatomic counterpart.

As hypothesized, using bone samples from regions proximal to the resection plane resulted in poorer correlations than those immediately distal to the humeral head resection. Clinically, this suggests that assessments of the bone quality from the resected

Table III
Mean (standard deviation) of Pearson's coefficients of correlation between each sample region and the distal support region that lies 20-50 mm beneath the humeral head resection, broken down as per sample slice depth, anatomic region and pooling technique, as well as subject osteoarthritis classification.

Pearson's coefficient of correlation with the distal support region (20-50 mm)					
Sample slice	Anatomic region	Pooled demographics	Nonarthritic	B2 OA	Symmetric OA
		Mean (SD)	Mean (SD)	Mean (SD)	Mean (SD)
5-10 mm above resection	Anterior	0.23 (0.11)	0.13 (0.13)	0.04 (0.16)	0.56 (0.10)
	Posterior	0.22 (0.10)	0.30 (0.15)	0.35 (0.11)	0.47 (0.08)
	Medial	0.37 (0.05)	0.17 (0.15)	0.39 (0.11)	0.51 (0.06)
	Lateral	0.23 (0.12)	0.21 (0.15)	0.23 (0.13)	0.58 (0.07)
	Central	0.25 (0.10)	0.35 (0.14)	0.25 (0.15)	0.50 (0.05)
	All pooled	0.26 (0.11)	0.23 (0.16)	0.25 (0.18)	0.52 (0.08)
	Anatomically paired	0.28 (0.11)	0.22 (0.16)	0.25 (0.18)	0.55 (0.08)
0-5 mm above resection	Anterior	0.25 (0.11)	0.23 (0.14)	−0.03 (0.20)	0.57 (0.07)
	Posterior	0.33 (0.11)	0.32 (0.16)	0.54 (0.10)	0.54 (0.07)
	Medial	0.29 (0.10)	0.30 (0.14)	0.33 (0.12)	0.43 (0.08)
	Lateral	0.25 (0.15)	0.31 (0.15)	0.39 (0.10)	0.57 (0.08)
	Central	0.23 (0.15)	0.33 (0.15)	0.45 (0.14)	0.56 (0.08)
	All pooled	0.27 (0.13)	0.30 (0.15)	0.33 (0.24)	0.53 (0.09)
	Anatomically paired	0.30 (0.14)	0.29 (0.14)	0.39 (0.18)	0.55 (0.09)
0-5 mm below resection	Anterior	0.33 (0.10)	0.38 (0.15)	0.17 (0.21)	0.55 (0.08)
	Posterior	0.38 (0.14)	0.44 (0.15)	0.55 (0.11)	0.53 (0.10)
	Medial	0.44 (0.09)	0.39 (0.13)	0.40 (0.13)	0.59 (0.09)
	Lateral	0.34 (0.14)	0.44 (0.13)	0.61 (0.13)	0.46 (0.11)
	Central	0.36 (0.16)	0.49 (0.15)	0.53 (0.11)	0.59 (0.11)
	All pooled	0.37 (0.13)	0.43 (0.15)	0.45 (0.21)	0.54 (0.11)
	Anatomically paired	0.40 (0.13)	0.42 (0.15)	0.48 (0.14)	0.56 (0.10)
5-10 mm below resection	Anterior	0.39 (0.11)	0.41 (0.16)	0.24 (0.17)	0.56 (0.08)
	Posterior	0.48 (0.14)	0.49 (0.16)	0.56 (0.13)	0.66 (0.10)
	Medial	0.55 (0.08)	0.44 (0.10)	0.55 (0.12)	0.71 (0.10)
	Lateral	0.39 (0.11)	0.39 (0.13)	0.65 (0.14)	0.43 (0.10)
	Central	0.49 (0.15)	0.57 (0.13)	0.56 (0.14)	0.70 (0.09)
	All pooled	0.46 (0.14)	0.46 (0.15)	0.51 (0.20)	0.61 (0.14)
	Anatomically paired	0.48 (0.12)	0.47 (0.13)	0.54 (0.16)	0.62 (0.14)

humeral head yield little insight into the variations in bone quality where the implant is supported. In general, poorer correlations were observed with samples that were further away from the support region; however, this is also partially attributed to the overlapping of the support and sample regions when assessing bone beneath the resection. Although better correlations can be found by sampling the bone beneath the resection, it is important to consider the implications that the sampling method may have on the integrity of this region as it is also involved in supporting implant structures after arthroplasty.

It was also hypothesized that correlating each subsection of the bone through anatomically paired sample and support regions would yield stronger relationships than if any 1 subsection from the sample regions was compared with all sections from the support regions, and this too was found to be true. Although there were instances of some anatomic sample sections correlating moderately (0.3 < r < 0.7), or even strongly (r ≥ 0.7), with all of the support regions of the nonarthritic and type A OA populations, the same was not true for B2 OA subjects. Owing to the asymmetric nature of OA in the Walch-B2 population, the anterior region consistently produced weak correlations with all other anatomic sections. Given that B2 OA subjects are often candidates for shoulder arthroplasty, we advise against making inferences regarding the entire support region from any 1 anatomic site when sampling bone density.

However, the present results indicate that these regional disparities in apparent density attributed to local OA conditions can be overcome if each anatomic section sampled is only used to infer the trends in apparent density that exist in the same anatomic section of the support region. Simply put, inferences drawn about the quality of bone in the anterior region of the resection plane should only be considered for the anterior support region, not the posterior, lateral, medial, or central regions, and so on. This has implications for how

surgeons should perform and interpret their "thumb tests." It is recommended that surgeons use the bone beneath the humeral head resection when making their assessments and that they consider testing all anatomic quadrants of the resection to make inferences about each independently. For example, a soft anterior resection may indicate a softer anterior region further down the metaphysis but should not be considered when making inferences about the lateral metaphyseal bone quality.

As previously discussed, correlations between the apparent densities of the sample and support regions were found to decrease in strength as the distance between the two regions increased. This spatial relationship, coupled with the general decrease in bone density observed as you move distally down the humeral canal,[20] accounts for the poor correlation coefficients found with the distal support region (20-50 mm beneath the resection plane). However, studies have indicated that bone density diminishes in this more distal region,[20] which may suggest that the proximal support region (0-20 mm beneath the resection) plays a larger role in supporting an implant's fixation features, although this still requires direct investigation.

Bone density was chosen to assess bone quality in the present study because it can be assessed nondestructively, and it is well correlated with bone strength.[1] It is also commonly used to infer material properties when constructing *in silico* finite element models of joints for its strong linear relationship with cancellous bone's elastic modulus.[16,19,21] Previous assessments of bone density from different joints throughout the body have suggested that bone density is heterogenous on a more macroscopic joint-to-joint level.[5,6,8,14] Within the humerus, Diedrichs et al[5] demonstrated that proximal density is strongly correlated contralaterally, but they noted only poor-to-moderate correlations between ipsilateral proximal and distal humeral joint density. This investigation has

built on the reported microscopic internal density distribution of the proximal humerus[20] and provides surgeons with more context when assessing resection bone quality via assessments such as the "thumb test."

This investigation is the first to assess how well the apparent density of bone near the humeral head resection plane correlates with the cancellous bone that ultimately supports a humeral stem after implantation. Although the present findings benefit from a relatively large population of 98 subjects, this study is not without its limitations. The use of a cadaveric population as a nonarthritic control resulted in a slightly older nonarthritic population than either of the OA cohorts; however, all cohorts did have subjects with overlapping ages, and care was taken to ensure that cadaveric samples were "fresh frozen" to reduce the likelihood of bone degradation postmortem. In addition, the inclusion of clinical subjects necessitated the use of clinical CT scan resolutions as opposed to micro-CT. As a consequence, the mean slice thickness of the scans from which density was assessed was larger than it could have been, at 0.9 ± 0.3 mm, although this is far smaller than the average slice thickness (5 mm) of the regions of interest investigated and was a trade-off accepted to include a clinical shoulder arthroplasty population. The inclusion of populations of patients with OA that did ultimately undergo shoulder arthroplasty yielded important insights regarding the strength of correlations between anatomic regions, which would have been missed in nonarthritic or type A arthritic subjects alone.

The purpose of the present investigation was limited to assessing the strength of the correlation between cancellous bone density from multiple sites within the proximal humerus. Future work is needed to determine appropriate methods for quantifying this density intraoperatively and to determine the relationship, if any, that may exist between these density measures and primary implant fixation. The quantitative nature of such relationships could eventually be used to help identify which humeral implant type is best suited for a patient when objectively considering their bone quality.

Conclusions

When "thumb testing" or performing other intraoperative assessments of humeral bone quality, the strongest correlations between sampled and supporting bone density can be found by assessing each anatomic region (anterior, posterior, medial, lateral, central) independently and using the bone distal to the humeral head's resection plane to make the assessment. Assessments of bone quality at the resection surface correspond to the anatomic region in which the implant will seek primary fixation, be that central, peripheral, or a combination thereof. Any methods used to assess bone density beneath the humeral resection plane should exercise caution to avoid substantially compromising the metaphyseal bone that is left behind to support an implant post-arthroplasty.

Disclaimers:

Supplementary data

Supplementary data to this article can be found online at https://doi.org/10.1016/j.jseint.2020.12.001.

References

1. Ammann P, Rizzoli R. Bone strength and its determinants. Osteoporos Int 2003;14:13-8. https://doi.org/10.1007/s00198-002-1345-4.
2. Banse X, Devogelaer JP, Munting E, Delloye C, Cornu O, Grynpas M. Inhomogeneity of human vertebral cancellous bone: systematic density and structure patterns inside the vertebral body. Bone 2001;28:563-71.
3. Bohsali KI, Bois AJ, Wirth MA. Complications of shoulder arthroplasty. J Bone Joint Surg Am 2017;99:256-69. https://doi.org/10.2106/JBJS.16.00935.
4. Bohsali KI, Wirth MA, Rockwood CAJ. Complications of total shoulder arthroplasty. J Bone Joint Surg Am 2006;88:2279-92. https://doi.org/10.2106/JBJS.F.00125.
5. Diederichs G, Korner J, Goldhahn J, Linke B. Assessment of bone quality in the proximal humerus by measurement of the contralateral site: a cadaveric analyze. Arch Orthop Trauma Surg 2006;126:93-100. https://doi.org/10.1007/s00402-006-0103-z.
6. Eckstein F, Lochmüller EM, Lill CA, Kuhn V, Schneider E, Delling G, et al. Bone strength at clinically relevant sites displays substantial heterogeneity and is best predicted from site-specific bone densitometry. J Bone Miner Res 2002;17:162-71. https://doi.org/10.1359/jbmr.2002.17.1.162.
7. Farley KX, Wilson JM, Daly CA, Gottschalk MB, Wagner ER. The incidence of shoulder arthroplasty: rise and future projections compared to hip and knee arthroplasty. JSES Open Access 2019;3:244. https://doi.org/10.1016/j.jses.2019.10.047.
8. Groll O, Lochmüller EM, Bachmeier M, Willnecker J, Eckstein F. Precision and intersite correlation of bone densitometry at the radius, tibia and femur with peripheral quantitative CT. Skeletal Radiol 1999;28:696-702.
9. Hasan SS, Leith JM, Campbell B, Kapil R, mith KL, Matsen FA. Characteristics of unsatisfactory shoulder arthroplasties. J Shoulder Elbow Surg 2002;11:431-41. https://doi.org/10.1067/mse.2002.125806.
10. Hoppe S, Uhlmann M, Schwyn R, Suhm N, Benneker LM. Intraoperative mechanical measurement of bone quality with the DensiProbe. J Clin Densitom 2015;18:109-16. https://doi.org/10.1016/j.jocd.2014.06.002.
11. Hvid I, Christensen P, Søndergaard J, Christensen PB, Larsen CG. Compressive strength of tibial cancellous bone: Instron® and osteopenetrometer measurements in an autopsy material. Acta Orthop 1983;54:819-25.
12. Ivanoff CJ, Sennerby L, Lekholm U. Influence of mono- and bicortical anchorage on the integration of titanium implants: a study in the rabbit tibia. Int J Oral Maxillofac Surg 1996;25:229-35.
13. Kim SH, Wise BL, Zhang Y, Szabo RM. Increasing incidence of shoulder arthroplasty in the United States. J Bone Joint Surg 2011;93:2249-54. https://doi.org/10.2106/JBJS.J.01994.
14. Krappinger D, Roth T, Gschwentner M, Suckert A, Blauth M, Hengg C, et al. Preoperative assessment of the cancellous bone mineral density of the proximal humerus using CT data. Skeletal Radiol 2012;41:299-304. https://doi.org/10.1007/s00256-011-1174-7.
15. Lübbeke A, Rees JL, Barea C, Combescure C, Carr AJ, Silman AJ. International variation in shoulder arthroplasty: incidence, indication, type of procedure, and outcomes evaluation in 9 countries. Acta Orthop 2017;88:592-9. https://doi.org/10.1080/17453674.2017.1368884.
16. Morgan EF, Bayraktar HH, Keaveny TM. Trabecular bone modulus-density relationships depend on anatomic site. J Biomech 2003;36:897-904. https://doi.org/10.1016/S0021-9290(03)00071-X.
17. Moroder P, Ernstbrunner L, Zweiger C, Schatz M, Seitlinger G, Skursky R, et al. Short to mid-term results of stemless reverse shoulder arthroplasty in a selected patient population compared to a matched control group with stem. Int Orthop 2016;40:2115-20. https://doi.org/10.1007/s00264-016-3249-5.
18. Mueller MA, Hengg C, Hirschmann M, Schmid D, Sprecher C, Audigé L, et al. Mechanical torque measurement for in vivo quantification of bone strength in the proximal femur. Injury 2012;43:1712-7. https://doi.org/10.1016/j.injury.2012.06.014.
19. Razfar N, Reeves JM, Langohr DG, Willing R, Athwal GS, Johnson JA. Comparison of proximal humeral bone stresses between stemless, short stem, and standard stem length: a finite element analysis. J Shoulder Elbow Surg 2016;25:1076-83. https://doi.org/10.1016/j.jse.2015.11.011.
20. Reeves JM, Athwal GS, Johnson JA. An assessment of proximal humerus density with reference to stemless implants. J Shoulder Elbow Surg 2018;27:641-9. https://doi.org/10.1016/j.jse.2017.09.019.
21. Reeves JM, Athwal GS, Johnson JA, Langohr GDG. The effect of inhomogeneous trabecular stiffness relationship selection on finite element outcomes for shoulder arthroplasty. J Biomech Eng 2019;141:034501. https://doi.org/10.1115/1.4042172.
22. Reeves JM, Knowles NK, Athwal GS, Johnson JA. Methods for post-hoc quantitative CT bone density calibration: phantom-only and regression. J Biomech Eng 2018;140:1-6. https://doi.org/10.1115/1.4040122.
23. Schairer WW, Nwachukwu BU, Lyman S, Craig EV, Gulotta LV. National utilization of reverse total shoulder arthroplasty in the United States. J Shoulder Elbow Surg 2015;24:91-7. https://doi.org/10.1016/j.jse.2014.08.026.

24. Sneppen O, Christensen P, Larsen H, Vang PS. Mechanical testing of trabecular bone in knee replacement - development of an osteopenetrometer. Int Orthop 1981;5:251-6.

25. Suhm N, Haenni M, Schwyn R, Hirschmann M, Müller AM. Quantification of bone strength by intraoperative torque measurement: a technical note. Arch Orthop Trauma Surg 2008;128:613-20. https://doi.org/10.1007/s00402-008-0566-1.

26. Suhm N, Hengg C, Schwyn R, Windolf M, Quarz V, Hänni M. Mechanical torque measurement predicts load to implant cut-out: a biomechanical study investigating DHS® anchorage in femoral heads. Arch Orthop Trauma Surg 2007;127:469-74. https://doi.org/10.1007/s00402-006-0265-8.

27. Tassani S, Öhman C, Baleani M, Baruffaldi F, Viceconti M. Anisotropy and inhomogeneity of the trabecular structure can describe the mechanical strength of osteoarthritic cancellous bone. J Biomech 2010;43:1160-6. https://doi.org/10.1016/j.jbiomech.2009.11.034.

28. Tulner SAF, Zdravkovic V, Külling F, Jost B, Puskas GJ. Haptic assessment of bone quality in orthopedic surgery: no consensus but perspective for high training potential. Int J Med Educ 2017;8:437-8. https://doi.org/10.5116/ijme.5a38.168c.

29. Yamada M, Briot J, Pedrono A, Sans N, Mansat P, Mansat M, et al. Age- and gender-related distribution of bone tissue of osteoporotic humeral head using computed tomography. J Shoulder Elbow Surg 2007;16:596-602. https://doi.org/10.1016/j.jse.2007.01.006.